

4-Dimensional Trackers

27th January 2022

Contact Information:

Ryan Heller (rheller.fnal.gov)

Ariel Schwartzman (sch@slac.stanford.edu)

1 Introduction

Ariel Schwartzman, Ryan Heller, Valentina Maria Martina Cairo, Zhenyu Ye

Precision Timing information at the level of 10-30ps is a game changer for detectors at future collider experiments. For example, the ability to assign a time stamp with 30ps precision to particle tracks will allow to mitigate the impact of pileup at the High-Luminosity LHC (HL-LHC). With a time spread of the beam spot of approximately 180ps, a track time resolution of 30ps allows for a factor of 6 reduction in pileup.

Both ATLAS and CMS will incorporate dedicated fast-timing detector layers for the HL-LHC upgrade [1, 2]. Timing information will be even more important at future high energy, high luminosity hadron colliders with much higher levels of pileup. For example, one of the key challenges at a future 100 TeV p-p hadron collider will be the efficient reconstruction of charged particle tracks in an environment of unprecedented pileup density. A powerful way to address this challenge is by fully integrating timing with the 3-dimensional spatial information of pixel detectors. An integrated 4-dimensional tracker with track timing resolution at the levels of ~ 10 ps can drastically reduce the combinatorial challenge of track reconstruction at extremely high pileup densities [3].

While timing information will be critical to mitigate the impact of pileup, it is not the only way in which it will enhance the event reconstruction of future hadron and lepton colliders. Timing information offers completely new handles to detect and trigger on long-lived particles (LLP) [2, 4], expand the reach to search for new phenomena by providing new handles on the data [2], and enabling particle-ID capabilities for pion/kaon separation at low transverse momentum [2]. 4D devices with coarse timing capabilities at \sim ns level but with similar granularity as regular tracking devices at the other end of 4D phase space can complement the fast timing layers for an enhanced overall 4D tracking.

The optimal design of future 4D trackers will involve three key considerations: sensors with adequate spatial and time resolution, low power and low noise readout electronics, and overall detector layout, including material considerations. Significant research and development effort is required to understand how to best design 4D trackers and how all these aspects will impact physics performance.

The following sections describe specific considerations for the integration of timing within tracking detectors at various future collider detectors and upgrades of existing experiments.

1.1 Hadron colliders

Valentina Maria Martina Cairo, Ryan Heller, Jenni Ott

The High Luminosity phase of the LHC (HL-LHC), expected to start around 2029, will be the first collider where precision timing capabilities will be necessary in order to accurately reconstruct events. The HL-LHC will feature approximately 200 nearly simultaneous collisions each bunch crossing, dispersed over a few hundred picoseconds. To disentangle this complex environment, CMS and ATLAS are building precision timing layers that will timestamp each track with roughly 30 ps precision, enabling the separation of slightly out-of-time pileup tracks from the primary interaction. These timing detectors, the ATLAS High Granularity Timing Detector (HGTD) [1] and the CMS MIP Timing Detector (MTD) [2] in the forward regions will be based on novel Low Gain Avalanche Detectors (LGADs), thin silicon sensors with modest internal gain. Though these sensors provide precise time information, they can only achieve modest spatial segmentation of approximately 1 mm. Thus, the timing layers serve as precursors to true 4D trackers and as excellent first platforms for developing precision timing in collider environments.

The ATLAS and CMS trackers will also be upgraded to cope with the extreme conditions of the HL-LHC [5, 6]. Due to the high radiation dose in close proximity of the interaction point, the two innermost pixel layers of the ATLAS inner tracker (ITk) will need to be replaced during the course of the HL-LHC. The longer timescale of this replacement offers an additional opportunity to develop precision timing in the pixel layers as well, naturally complementing the HGTD in the forward region. Even a single pixel barrel layer with timing capabilities could afford a vast performance improvement and would also be a striking first demonstration of true 4D tracker. The pixel time resolution needed to substantially boost the ATLAS performance is still to be evaluated along with the impact of material introduced in the tracker, but detailed simulation studies are needed to evaluate the potential of such detector layout and eventually probe its feasibility.

The simplification provided by precision timing at the HL-LHC will have substantial impact for some of the most challenging and important physics analyses, including searches for Higgs pair production, measurement of missing energy, searches for long-lived particles, and particle identification (PID) in heavy ion collisions.

Beyond HL-LHC, one of the key challenges in the design of Future hadronic Circular Colliders (FCC-hh [7]) arises from a further increased number of pile-up events $O(1000)$, almost an order of magnitude more than at the HL-LHC. Track-finding and identification of vertices based on traditional 3D algorithms will be extremely difficult, making a very clear case for the usage of 4D technology in all tracking layers. Timing information at each layer allows only associating hits that are consistent in time, which will dramatically reduce the complexity in the extreme occupancy environment.

One important question to answer is what timing resolution is needed for a collider like the FCC. A key metric used is the effective pileup, which represents the mean number of vertices coincident with the primary interaction that cannot be resolved based on the available spatial or timing information. As shown in Fig. 1, extreme timing resolution of 5–10 ps per track is essential to keep the effective pileup low and prevent the merging of unrelated vertices.

At the same time, the higher energies and luminosities typical of the FCC-hh pose very stringent constraints on the detector design itself, for instance on the radiation hardness of the silicon modules, limiting either the lifetime of the inner detector or the suitable detector technologies. In the layouts under study [7], the beampipe is taken to have a radius of 20 mm. At the radius of the innermost tracker layers, 25 mm, the radiation levels expected after 30 ab^{-1} are of the order of a dose of 0.4 G Gy and a fluence of 6×10^{17} per cm^2 1 MeV neq. These are approximately 30 times (600 times) more intense than the environment at the HL-LHC (LHC). No existing tracker technologies

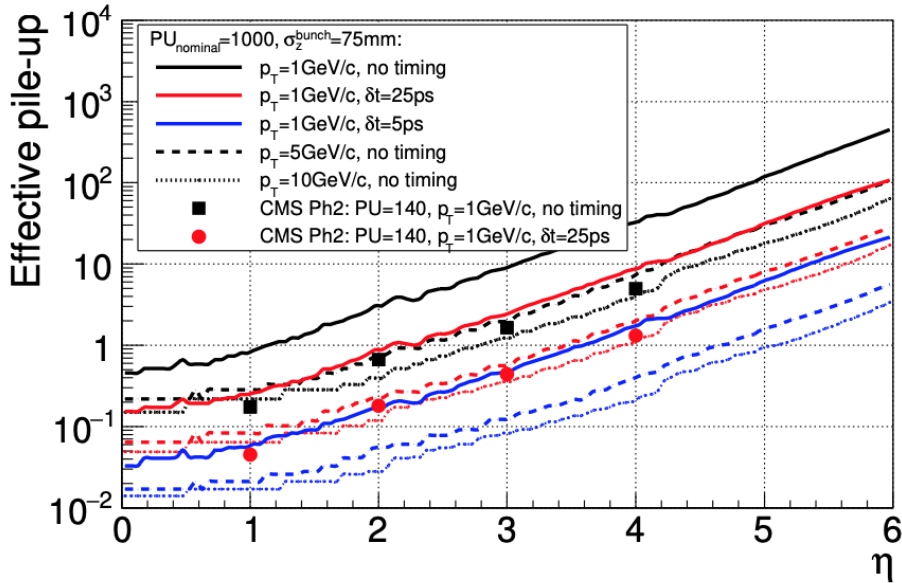


Figure 1: From Ref. [8]. An effective pile-up in the FCC-hh tracker. Several options of timing resolution per track in 3D vertexing are assumed: no timing (black), $\delta t = 25$ ps (red) and $\delta t = 5$ ps (blue). Several p_T values are shown: 1 GeV/c (solid), 5 GeV/c (dashed) and 10 GeV/c (dotted). For reference the effective pile-up for CMS Phase 2 layout, $p_T = 1$ GeV/c and nominal pile-up=140 is added.

85 can satisfy these requirements, and dedicated RD efforts targeting extreme timing resolutions and
 86 radiation hardness must be pursued.

87 1.2 e^+e^- colliders: ILC, CLIC, C³ (?)

88 Valentina Maria Martina Cairo, Lucie Linssen

89 The usage of 4D tracking technology at e^+e^- colliders is subject to very different conditions
 90 compared to that of experiments at hadron machines: both the numbers of collisions per beam
 91 crossing and the radiation levels are orders of magnitude lower, but the physics measurements are
 92 normally targeting very high precision, imposing track parameter resolutions to be extremely good,
 93 thus requiring very low passive material in the vertexing and tracking detectors.

94 Most of the studies performed so far focus on the usage of time at the ns resolution level as
 95 part of the object reconstruction chain, while studies of potential applications of precision timing at
 96 the ps level are still to be further investigated in e^+e^- colliders. Both aspects will be summarised
 97 below.

98 The International Linear Collider (ILC) [9] is a proposed 20 km e^+e^- linear collider at the
 99 energy frontier, with a initial baseline center-of- mass energy of 250 GeV. Two detector concepts
 100 have been studied at the ILC: the Silicon Detector (SiD) and the International Large Detector
 101 (ILD).

102 SiD is a compact detector based on a powerful silicon pixel vertex detector, silicon tracking,
 103 silicon-tungsten electromagnetic calorimetry (ECAL) and highly segmented hadronic calorimetry
 104 (HCAL). SiD also incorporates a 5T solenoid, iron flux return, and a muon identification system.
 105 The choice of silicon detectors for tracking and vertexing ensures that SiD is robust with respect

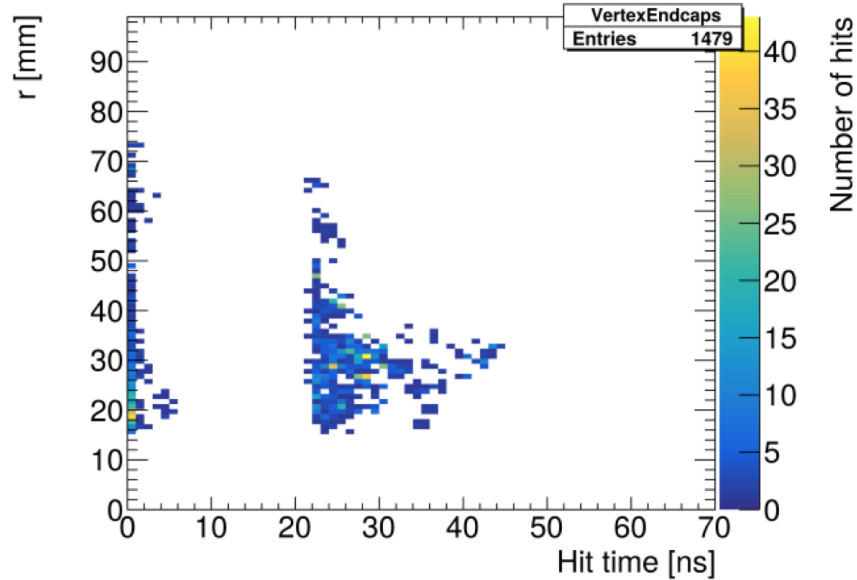


Figure 2: From Ref. [10]. The time distribution of beam background hits in the SiD Vertex Detector Endcap.

106 to beam backgrounds or beam loss, provides superior charged-particle momentum resolution, and
 107 eliminates out-of-time tracks and backgrounds. The recent developments in fast-timing detectors
 108 could bring in improvements to the SiD layout, as described in Ref. [10]. Timing layers with
 109 resolutions at the level of the nanosecond could be used in the HCAL to help suppress backgrounds.
 110 Fig. 2 shows the timing distribution of the beam background hits displaying the collision and then
 111 with a clear separation the backgrounds hits from a back-splash from the forward instrumentation.

112 Better time resolutions would instead make it possible to exploit time-of-flight (TOF) for low-
 113 momentum particle identification (PID) if timing layers were added to the tracking system or in
 114 between the tracker and the ECAL. Fig. 3 shows that, in SiD, a TOF system with time resolution
 115 of 10 ps allows for PID up to a momenta of a few GeV.

116 The ILD concept has been designed as a multi-purpose detector for optimal particle-flow (PFA)
 117 performance. Its tracking systems differs from the SiD one: a high-precision vertex detector is
 118 followed by a hybrid tracking system, realised as a combination of silicon tracking with a time-
 119 projection chamber (TPC). The complete system, along with a calorimeter, is located inside a 3.5
 120 T solenoid.

121 Particle identification in the ILD can be carried out by the TPC using dE/dx information but
 122 studies have been conducted [11] on the possibility of improving PID via a TOF system. As a proof
 123 of concept a possible TOF estimator is computed, which uses the first ten calorimeter hits in the
 124 ECAL that are closest to the straight line, resulting from extrapolation of the particle's momentum
 125 into the calorimeter, assuming an individual time resolution of 100 ps per hit. Fig. 4 shows the
 126 complementary between dE/dx and TOF information at the ILD.

127 The momentum range in which the particle identification using TOF is effective depends on the
 128 time resolution. More detailed studies [12] show that smaller time resolutions do boost the PID
 129 reach in the low momentum regime, but the momentum range covered via TOF for PID remains
 130 limited, as one can see in Fig. 5. Dedicated PID detectors would have to be installed to discriminate
 131 pions from kaons at high momenta and more information about related studies can be found in [?].

132 The Compact Linear Collider (CLIC) [13, 14] is another proposed e^+e^- machine featuring a

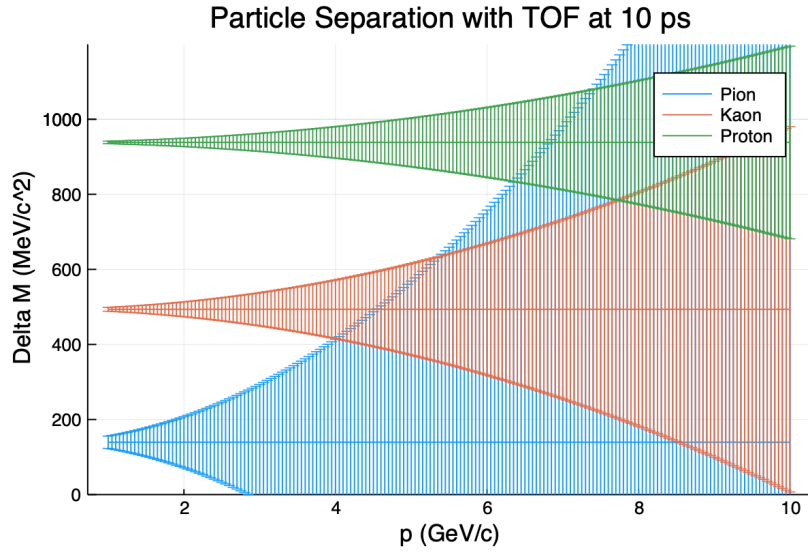


Figure 3: From Ref. [10]. Mass resolution for a time-of-flight system with a performance of 10 ps in SiD.

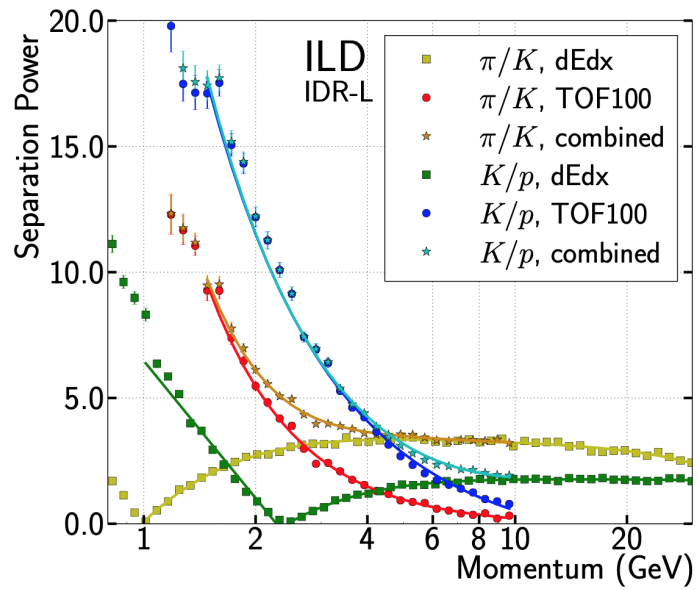


Figure 4: From Ref. [11]. Particle separation power for π/k and K/p based on the dE/dx measurement in the TPC and on a time-of-flight estimator from the first ten ECAL layers. The separation power obtained when the information from the two systems is combined is also shown.

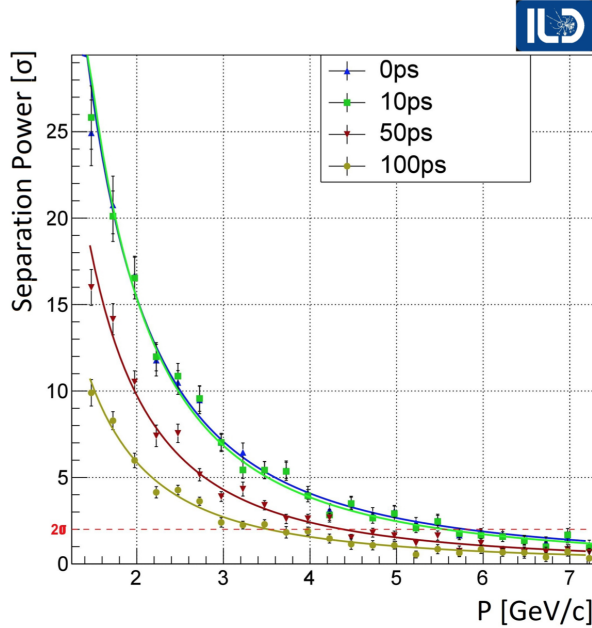


Figure 5: From Ref. [12]. Separation power between kaons and pions as a function of momentum assuming different time resolutions for a time-of-flight system in ILD.

133 future multi-TeV collider.

134 The CLICdet detector concept is derived from the ILC detector concepts, adapted to the higher
 135 energies and background conditions at CLIC. A fully silicon-based tracking system is foreseen.
 136 Bunch trains at CLIC occur at a rate of 50 Hz, with each bunch train comprising 312 bunch crossing
 137 separated by 0.5 ns. Triggerless readout once per bunch train is foreseen. To ensure low occupancies,
 138 e.g. the required maximum pixel size in the vertex detector is $25 \times 25 \mu m^2$. The timing requirements
 139 at CLIC are driven by the levels to which the background degrades the physics performance of the
 140 detector. Low occupancies allow for efficient track reconstruction. Accurate track information is
 141 used in the subsequent particle-flow reconstruction step, where all charge and neutral particles
 142 are reconstructed, including particles from beam-induced background. By requiring a hit-time
 143 resolution below 5 ns for the vertex and tracking detectors, and 1 ns resolution for calorimeter
 144 hits, all the particle-flow objects have sub-ns time resolution (see Section 2.5 in Ref. [13]). This
 145 information is used to remove particles from beam-induced background via momentum and timing
 146 cuts as a function of the angular region and of the particle type. As a result, CLIC physics
 147 performance is essentially preserved at all foreseen centre-of-mass energies.

148 Dedicated 4D tracking studies with ps-level resolution in some of the tracking layers have not
 149 yet been performed in CLIC. It has to be noted though that CLIC assumes to run at 380 GeV and
 150 above, thus the impact of fast timing in a TOF system is expected to have less added value for
 151 CLIC than for e^+e^- collisions at lower centre-of-mass energies.

152 1.3 Muon Collider

153 Hannsjörg Weber, Sergo Jindariani

154 Experiments at muon colliders have huge potential. A muon collider as a Higgs factory might
 155 allow to directly measure the mass and width of the Higgs boson at highest precision [15]. On
 156 the other hand, muon colliders have a potential to achieve collision energies of tens of TeV with a

157 relatively small size for a collider ring, thus reaching way further than e^+e^- colliders and having
158 a physics reach on-par with hadron colliders with hundreds of TeV in collision energy [16]. The
159 current timeline to complete the accelerator R&D and be ready for the construction of a muon
160 collider is estimated to be earliest in the latter part of the 2030s [17].

161 The major challenge for a muon collider experiment is that muons are unstable particles and
162 naturally decay. The decaying muons within the colliding beams will create, for each beam crossing,
163 a spray of hundreds of million particles entering a muon collider experiment. Out of those, an order
164 of a million particles is charged. This multiplicity of particles entering the detector volume is
165 expected after the muon collider experiment has already been shielded by so-called nozzles in the
166 forward region, blocking the volume of $|\eta| \lesssim 2.5$. The background induced by these particles is
167 commonly referred to as the beam-induced background (BIB) [18]. The BIB primarily consists of
168 low energy photons and neutrons with a small fraction of charged hadrons, muons and electrons
169 also present.

170 The presence of the BIB puts stringent requirements on a tracking detector. Firstly, the high
171 number of particles entering the detector region leads to high levels of radiation and thus detectors
172 need to be radiation hard, similarly to the detectors at hadron colliders. Secondly, hits produced
173 by the BIB particles complicate data readout and make track reconstruction at the muon collider
174 a very challenging task.

175 Yet, as the decay of muons is a stochastic process, several advantageous design aspects for
176 tracking detectors can be thought of to suppress the impact of the BIB. Most of the BIB particles
177 enter the detector from the two forward regions and do not originate in the collision area. Precise
178 timing of detector hits would be able to reduce the BIB by a large fraction as we only need to
179 consider hits consistent with the collision time. Furthermore, if timing of the hits can be correlated
180 among adjacent layers of a tracking detector, a further filtering can be done by only considering
181 hits consistent with being produced by the same particle. Initial studies indicate that single hit
182 resolutions of 20-30 ps are sufficient to reduce the BIB to a manageable level. Additional suppression
183 can be achieved if the tracker can obtain directional information, as for example is being done with
184 the p_T modules of the CMS outer tracker upgrade for the HL-LHC [19]. Besides the requirements
185 of precise timing and directionality, also a high spatial resolution is needed to achieve a low detector
186 occupancy. Simulation studies show that small pixels at a size of about $(25 \mu\text{m})^2$ are needed at the
187 innermost layers of a tracking detector while even at the outermost layers strips with length of at
188 most few cm are required [20].

189 These requirements on small pixels/strips with precise timing and directional information will
190 allow to not only handle the BIB, but will also enable a muon collider experiment to take high
191 quality data for precision measurements and searches for new physics at highest energies [21].
192 Therefore, there is a high need of R&D efforts towards 4D (and 5D) tracking within the muon
193 collider community.

194 1.4 Electron Ion Collider

195 Zhenyu Ye

196 The Electron-Ion Collider (EIC) [1] is a new accelerator facility to be built at Brookhaven
197 National Laboratory in the United States. In 2031, the machine will begin colliding high-energy
198 electron beams with high-energy proton and ion beams to study the spatial and spin structure of
199 nucleons and nuclei. Due to the small ep and eA cross-sections, the collision rate at the EIC will
200 be 500 kHz or less with a total particle production rate of about 4 million per second. Therefore,
201 the requirement on the irradiation tolerance and occupancy of the detectors at the EIC will be
202 considerably relaxed than those at the hadron colliders.

203 AC-coupled LGADs have been widely included in the submitted EIC detector proposals. In the
 204 barrel (endcap) region, precise timing and spatial information will be provided by single (double)
 205 layer of AC-LGADs for particle identification and track reconstruction, while in the far-forward
 206 (p/A-going) direction, AC-LGADs will be used to detect high-momentum hadrons near the beam
 207 line. These detectors need to provide a single hit timing resolution better than 30 ps and depending
 208 on the location a single hit spatial resolution between 15 to 150 μm . The detector designs need to
 209 incorporate low material budgets, e.g., $\sim 1\%$ X_0 per layer in the barrel region. These impose a great
 210 challenge to the performance of AC-LGAD sensors, front-end readout ASIC, off-detector electronics,
 211 as well as the mechanical and cooling system design. A R&D project has been established to develop
 212 a common approach for these detectors so that they can share the same design to the extent possible.

213 [1] Science Requirements and Detector Concepts for the Electron-Ion Collider: EIC Yellow Re-
 214 port, BNL-220990-2021-FORE, JLAB-PHY-21-3198, LA-UR-21-20953, arXiv:2103.05419 (2021).

215 **2 Sensor technologies**

216 Simone Mazza, Ryan Heller, Ron Lipton, Gabriele Giacomini, Doug Berry, Jennifer Ott, Valentina
 217 Maria Martina Cairo

218 **2.1 Advanced LGAD designs**

219 LGADs, AC-LGADs, Trench-isolated LGADs, Buried Gain LGADs, Deep Junction LGADs, 3D
 220 The most prominent class of 4D sensors proposed for future trackers are based on an evolution
 221 from Low-Gain Avalanche Diode sensors developed for the HL-LHC. LGADs are thin silicon sensors
 222 with modest (~ 5 -50) intrinsic gain provided by a moderately doped p+ multiplication layer, and
 223 achieve 30 ps or better time resolution. Standard LGADs, however, feature mm scale pads and rely
 224 on Junction Termination Extensions to interrupt the gain layer between channels, which introduces
 225 inactive regions. As a result, LGADs cannot be simply miniaturized to a pitch appropriate for
 226 tracking. Several sensor concepts have been proposed and demonstrated to make LGAD sensors
 227 suitable for tracking, in addition to providing excellent timing resolution. In the following sections
 228 several innovative LGAD designs to achieve high granularity will be introduced.

229 **2.1.1 AC-coupled LGADs**

230 Ryan: Move some of description from general section here, add some test beam results. Simone: I
 231 had a stab at it, please check

232 The most advanced high granularity LGAD design so far is the AC-coupled LGAD (AC-LGAD).
 233 In contrast to standard LGADs, AC-LGADs feature a continuous gain layer and a more resistive n+
 234 surface layer. The signal is capacitively (AC-) coupled over the equally continuous dielectric to the
 235 metal readout electrodes. Because the gain layer is uninterrupted, AC-LGADs achieve a fill factor
 236 of 100%, and electrodes can be designed with smaller pitch and size than standard LGADs. A key
 237 feature of AC-LGADs, brought on by the common gain and n+ layer, is the signal sharing between
 238 electrodes, which can be used to obtain position measurements with resolution much smaller than
 239 (bin size)/ $\sqrt{12}$. Hence, one major advantage of AC-LGADs is that they can obtain the spatial
 240 resolution necessary for future colliders with a coarser pitch and thus a reduced number of readout
 241 channels.

242 Recent test beam measurements have demonstrated that AC-LGADs can achieve simultaneous
 243 30 ps and 5 μm resolution with strips of pitch 100-200 μm [22]. This spatial resolution represents a
 244 factor of 5-10 improvement beyond what would be obtained in binary readout, thanks to the sharing

245 of signals between adjacent channels. Other studies have demonstrated similar performance [23]
246 [24].

247 **Simone/Jenni: add some UCSC laser results and simulations, non conventional geom-**
248 **etry.**

249 AC-LGADs have several parameters that can be tuned to optimize the sensor response to the
250 specific application. The geometry of the electrodes in terms of pitch and pad dimension is the most
251 important one, however also the n+ sheet resistivity and the thickness of the dielectric between n+
252 and metal electrodes influence the charge sharing mechanism, as well as signal characteristics such
253 as the undershoot (recovery to baseline) after a signal. All of the AC-LGAD parameters affect the
254 final performance of the sensor, therefore it is necessary to balance these properties to achieve the
255 best timing and spatial resolution with respect to the channel density and occupancy.

256 For optimizing the sensor design in terms of the abovementioned parameters, simulation with
257 TCAD software, such as Silvaco or Synopsys Sentaurus, is an important tool. On the other hand,
258 experimental data from prototype sensors serves as a vital input to simulation models in order for
259 them to provide a good representation of the observed sensor performance, and have predictive
260 power for future devices.

261 As neither the gain layer, n+ layer nor dielectric have significant underlying structure, it is
262 possible to arrange the metal of the AC-LGAD readout electrodes in any desired shape and size.
263 This allows to optimize the electrode geometry to tune the charge sharing to the specific application.
264 For example, circular or cross-shaped metal electrodes, instead of squares, could further improve
265 position resolution through the utilization of advanced reconstruction algorithms. Electrodes can
266 also be arranged on a triangular grid, instead of square or rectangular alignment, to further enhance
267 charge sharing. Furthermore, electrodes can be shaped to have different charge sharing in the X
268 and Y direction (e.g. micro-strips) to optimize the channel density to the sensor resolution in both
269 directions. A recent sensor production by FBK allows systematic evaluation of various electrode
270 patterns and geometries. Another proof of principle to obtain different metal electrode geometries,
271 featuring a modification process of metal electrodes executed at BNL, was made [25]. The procedure
272 was successful, showing that the top metal geometry of AC-LGADs can be modified. Thus, a
273 universal metal design could be produced and subsequently etched to meet the requirements of any
274 specific application.

275 **2.1.2 Buried Layer LGADs**

276 Radiation campaigns showed that LGADs with deep and narrow gain layers are radiation harder
277 than LGADs featuring shallower and broader gain layers. Gain layers are generally obtained by
278 means of ion implantations which can implant boron at a maximum depth of about 2 μm using very
279 high and not easily available implantation energies. Furthermore, deeper implants are generally
280 broader than shallower implants. A way to circumvent the problem, at the expense of a complication
281 in the process, is to implant the boron layer at low energy and then to bury it under a few microns
282 of epitaxial layer, obtaining in this way a deep and narrow gain layer (if high thermal cycles are
283 avoided in the subsequent process. The method can be applied to either standard DC-coupled
284 LGADs or AC-LGADs. A first fabrication has been completed but suffered from a high leakage
285 current due to a poor epitaxial deposition. Another fabrication is on-going.

286 **2.1.3 Trench-insulated LGADs**

287 FBK group

288 A way to avoid AC-LGADs and still have a high fill-factor in fine-pitch devices is to use narrow

289 trenches, filled with insulator, to separate the pixels (or strips). The deployment of such trenches
290 all around the electrodes allows to get rid of the JTE, to bring the gain layer closer to the edge of
291 the n-plus implants, and to bring the pixels close together. Dead areas of a few microns have been
292 demonstrated in the first FBK prototype productions [26].

293 **2.1.4 Double Sided LGADs for 5D Tracking**

294 The Double Sided LGAD (DS-LGAD) adds a readout layer to the p-side of the LGAD structure.
295 This allows for double-sided readout with the p side reading out the slower-drifting holes. For a
296 device with the bulk thickness large compared to the pixel pitch the p-side readout can function as a
297 mini time projection chamber with the drift time providing information on the depth of origin of the
298 charge cloud. The signal p-side collects two components, holes from the primary ionization followed
299 by the larger number of holes generated at the gain layer. This provides a unique signature of the
300 pattern of charge deposit within the device (figure AAAA). The fast rise signal can be read by a
301 large area cathode, limiting the number of complex, power hungry fast amplifiers and digitizers. The
302 p-side provides a large, slower signals that can be read out with electronics with lower complexity
303 and power consumption.

304 The characteristics of the thick ($> 5 \times pitch$) DS-LGAD are sensitive to the interplay between
305 the device thickness, gain layer location and doping, and the applied voltage. In a buried layer
306 device the depth and doping of the gain layer sets the operating point and the drift field. These can
307 be tuned to achieve the required characteristics. Diffusion width and time of arrival of the holes
308 from gain layer amplification can then be used to provide excellent position and good track angle
309 resolution. Operation will be a compromise as these thicker devices will have worse time resolution
310 than thin LGADs and may be more sensitive to radiation effects on doping levels.

311 **2.1.5 Deep-Junction LGADs**

312 Simone (UCSC)

313 The “Deep-Junction LGAD” (DJ-LGAD) [27] is a new approach to the application of controlled
314 impact-ionization gain within a silicon diode sensor. The term “deep-junction” arises from the use
315 of a p-n semiconductor junction buried several microns below the surface of the device. The buried
316 junction is formed by abutting thin, highly-doped p+ and n+ layers, with the doping density
317 chosen to create electric fields large enough to generate impact ionization gain in the narrow buried
318 junction region. Additionally, the doping densities chosen for the p+ and n+ layers are balanced so
319 that when the sensor is fully depleted, the electric field outside of the junction region, while large
320 enough to saturate the carrier drift velocity, is significantly less than that require to create impact
321 ionization gain. This preserves the electrostatic stability at the segmented surface of the detector,
322 thus in principle permitting the production of DC-coupled LGADs with arbitrarily fine granularity.
323 No JTE structure is required for a DJ-LGAD array, as the buried gain layer ensures a uniform gain
324 performance across channels. The DJ-LGAD approach is seen to hold significant promise towards
325 the development of a highly-pixelated DC-coupled silicon diode sensor with substantial internal
326 gain and precise temporal resolution.

327 **2.1.6 Thin LGADs**

328 Simone (UCSC)

329 Thin sensors can be a useful technology to apply in very high radiation environment [28, 29].
330 In the late years a saturation of the charge trapping effect in silicon was observed [30]. However
331 at a fluence of $10^{17} - 10^{18}$ a standard 300 um silicon detector would still need several thousand

332 volts to deplete. For a thin sensor instead the full depletion at very high fluence can happen at
333 much lower voltages: 500 V of full depletion for a 50 μm sensor at 10^{17} . The collected charge for
334 thin sensors, however, would be too small to be efficiently detected by readout electronics. Thin
335 LGADs can be used thanks to the intrinsic charge multiplication, it was shown that sufficient gain
336 is observed until a few 10^{15} for time resolution measurements purposes but less gain is necessary
337 for hit detection only. Furthermore at high fluences gain in the bulk “p” region of the sensor can be
338 activated by increasing the bias voltage applied to the sensor. These statements gives an indication
339 of the radiation hardness properties of thin LGADs even at extreme fluences for hit detection. An
340 example of extreme fluence would be a tracking system very close to the interaction point in future
341 hadron colliders.

342 2.2 3D silicon sensors

343 Adriano Lai

344 Since their introduction in 1997 [31], sensors with three-dimensional electrodes (3D silicon
345 sensors) have been widely consolidated, being presently used in LHC experiments (CMS-PPS [32],
346 ATLAS-IBL [33]). Such sensors are characterised by cylindrical electrodes, penetrating the bulk
347 material, perpendicularly to the surface. 3D sensors with cylindrical electrodes have shown to
348 maintain high performance up to fluence close to 10^{17} 1 MeV neq/cm² [34,35]. The specific structure
349 of 3D sensors decouples the charge carrier drift distance from the sensor thickness. This allows
350 reduced inter-electrode spacing, thus minimising the probability of charge trapping by defects
351 generated by radiation. The geometry of 3D sensors is also very beneficial in terms of timing
352 performance. Very short collection times can be achieved without reducing the substrate thickness,
353 thus preserving the signal amplitude. The fact that the charge carriers are collected perpendicularly
354 to the sensor thickness minimises time uncertainties due to nonuniform ionisation density, delta rays
355 and charge carrier diffusion. Moreover, the vertical geometry of the electrodes allows a large margin
356 of choice in defining the pixel layout and the structure of the sensitive volume. This property can
357 be exploited in minimising unevenness in the electric field and increasing the uniformity in signal
358 response to obtain very high time resolutions. In the last years, results have been obtained by
359 the TimeSPOT collaboration [36,37], which show that by proper design of the sensor layout and
360 electrode geometry, the time resolution can be pushed well below 20 ps at room temperature. The
361 measured resolution is limited by the front-end electronics performance, while the sensor intrinsic
362 resolution is estimated around 10 ps. TimeSPOT sensors have been designed and fabricated in
363 a so-called 3D-trench geometry (linear parallel trenches for bias and collection electrodes). The
364 sensitive pixel volume size is $55 \times 55 \times 150 \mu\text{m}^3$ and is operated at a bias voltage around 100 V. A
365 general feature of 3D sensors are the dead areas represented by the biasing and collecting electrodes,
366 which introduce a detection inefficiency for particles traveling perpendicular to the sensor surface.
367 This effect has been studied in detail for 3D silicon sensors based on columnar geometry, which
368 are used in the ATLAS IBL [38]. Test beam studies have been recently performed also on 3D-
369 trench TimeSPOT pixels. Preliminary results show that an efficiency of almost 100% is reached
370 for tracks with 20 degrees inclination, while maintaining the same time resolution. Dedicated
371 integrated CMOS 28 nm read-out electronics is under development. A small prototype ASIC,
372 named Timespot1, featuring a matrix of 1024 pixels and integrating one TDC per pixel channel
373 has been recently tested being capable of a time resolution around 30 ps on the full read-out
374 chain [39].

375 2.3 MAPS

376 Fine spatial resolution and course time resolution: CMOS MAPS. Coordinate with CMOS paper
377 Valentina: for Malta, there is public material here we can use as a reference (including a section
378 on timing) <https://twiki.cern.ch/twiki/bin/viewauth/Atlas/MaltaApprovedPlots>
379 and also this CERN EP RD seminar: [https://indico.cern.ch/event/1074066/2-measurement-](https://indico.cern.ch/event/1074066/2-measurement-results-from-fas)
380 [results-from-fas](https://indico.cern.ch/event/1074066/2-measurement-results-from-fas)

381 2.4 Induced Current Detectors

382 An induced current detector uses the same sensor as a traditional silicon detector but utilizes small
383 pixel pitch and 3D integration (3DIC) techniques to create a low-capacitance pixel unit cell and
384 readout chain. This not only limits the amount of noise in the system but also enables the detection
385 of the induced current as described by the Schokley-Ramo theorem [40, 41]. The Schokley-Ramo
386 current is the current induced at the readout electrode from mobile charge carriers within the sensor.
387 It has a very fast rising edge (~ 15 ps) [42] and can be used to precisely timestamp track hits.
388 The Schokley-Ramo current is dependent on the weighting field within the sensor and the depth of
389 charge deposition. As a direct result, it has a complicated bi-polar signal shape that integrates to
390 zero over the course of several nanoseconds. This signal combined with the drift current creates a
391 pulse shape that is dependent on the charged particle's angle of incidence.

392 A detector that is sensitive to the effects of the Schokley-Ramo current has two critical features:
393 precise (~ 15 ps) time resolution and angle of incidence information [43]. The precise time resolution
394 is useful in many different collider experiments and can be used for either vertexing or particle
395 identification via a time-of-flight (TOF) measurement. The angular information is a more novel
396 feature but still useful feature. First it can be used to quickly identify particles with large transverse
397 momentum (p_T) for an L1 trigger, as high- p_T particles have high angles of incidence. Second it
398 can be used to greatly increase the speed of track reconstruction because the angular information
399 greatly reduces the number of pixel hits that must be considered when track seeds are generated.
400 These capabilities make it a very attractive detector technology for future collider experiments and
401 requires the continued investment in advanced ASIC design and 3DIC techniques.

402 2.5 Comparison of sensor technologies

403 Tradeoffs for different sensors: high occupancy? material budget? rad hardness?

404 3 Electronics

405 While readout prototypes for the timing detectors at the HL-LHC upgrades have demonstrated
406 performance in line with requirements, applying similar techniques in trackers presents several
407 challenges. High granularity requirement of future trackers will require readout ASICs with smaller
408 pixel sizes compared to present generation, maintaining power consumption levels similar to present
409 designs without timing extraction. Accommodating the additional required electronics for timing
410 extraction, i.e. Time to Digital Converters (TDCs) [44] and memories together with the typical
411 pixel circuitry of present trackers, in pixels at pitches on the order of tens of microns will require the
412 adoption of deeper low power and fast technology nodes beyond 65nm. The entire pixel electronics
413 will need to be designed with low power techniques and with novel timing extraction architecture.
414 In addition, the high luminosity of future hadron colliders will require trackers capable to survive
415 in extreme radiation environments (accumulating a dose of up to 30 GRad and 10^{18} neutrons/cm²)

416 Because of these aspects, state-of-the-art low power CMOS and Bi-CMOS technology targeted for
417 the mmW communication industry are of particular interest. These includes FDSOI technologies
418 which could potentially open a path to monolithic readouts at very fine pitch. These technologies
419 are also of interest in other HEP applications for their demonstrated performance at deep cryogenic
420 temperatures.

421 **This might be suitable here**

422 It is important to stress that the read-out philosophy of standard PIN silicon sensors and
423 UFSD is different. In PIN sensors, the maximum current happens just after the passage of the
424 particle while in UFSD the current increases for the duration of the electron drift time, then there
425 is a plateau, and finally decreases. This peculiar signal shape limits the useful bandwidth of the
426 amplifier. The amplifier bandwidth affects both noise and slope and, ideally, the higher BW the
427 lower the jitter. However, the intrinsic time response of UFSD sensors sets the upper limit to the
428 maximum reachable slope that the analog output can exhibit. As a consequence, the bandwidth
429 should be chosen to be the minimum value that retains the intrinsic sensor speed while keeping the
430 noise low. The bandwidth defines the signal shaping of the front-end and its optimum value for
431 timing is obtained when the amplifier shaping time equals the sensor peaking time.

432 **Useful text to incorporate?**

433 Advances in detector technology and the direction of HEP experiments and applications require
434 the development of new specialized readout electronics. Experimental demands include some com-
435 bination of high rep rates (order of ns dead time), below 10 ps time of arrival (TOA) resolution,
436 low power (between 0.1 mW and 1 mW per channel), and high dynamic range (for some specific
437 application up to a few 1000s).

438 **3.1 Current timing chips**

439 brief discussion of ALTIROC, ETROC (Ryan), capabilities and limitations

440 **3.2 FAST family of ASICs**

441 **Keep or remove?**

442 In the past several years the FAST effort had the goal of designing an ASICs tailored to the read-
443 out of Ultra-Fast Silicon Detector. TOFFEE [45], the first prototype, has been produced in 2016,
444 FAST1 in 2018 [46], and FAST2 [47] in 2020. This family of ASICs aims to provide a 25 ps time
445 resolution with rates up to 200 MHz and has been designed in a 110 nm CMOS commercial tech-
446 nology node. In every iteration of the production the architecture has been improved to optimize
447 the chip performance. Starting from FAST2 a analog-only version of the chip have been produced.
448 The next foreseen production is FAST3, which is based on the studies performed on FAST2 with
449 expand linearity of the output dynamic range. In parallel to FAST3, the ASIC UFSD_ALCOR has
450 been designed. It includes the optimized front-end stage used in FAST3_Analog, a discriminator
451 stage, time to digital converter (TDC), and a digital control unit. Each channel can measure the
452 Time of Arrivals (ToA) and Time of Threshold (ToT) of a pulse signal with a least significant bit
453 of 25 ps. FAST3 and UFSD_ALCOR are almost completed and will be manufactured in the first
454 half of 2022.

455 **3.3 SiGe amplifiers**

456 A possible path to achieve O(10 ps) time resolution is an integrated chip using Silicon Germanium
457 (SiGe) technology. Using DoE SBIR funding, Anadyne, Inc. in collaboration with University of
458 California Santa Cruz has developed a prototype SiGe front end readout chip optimized for low

459 power and timing resolution, with 0.5 mW per channel (front end and discriminator) while retaining
460 10 ps of timing resolution for 5 fC of injected charge. In the process some insight was developed
461 into the challenges and potential performance of SiGe front end ASICs for future R&D effort.
462 The developed single pre-amplifier stage and what is effectively a Time Over Threshold (TOT)
463 discriminator topology is suitable for low repetition rate and quiescent power and sub 10 ps timing
464 resolution applications. Some practical considerations for selecting a process for future R&D include
465 the size and power efficiency of the CMOS transistors for the back-end electronics and diminishing
466 performance gains of higher speed SiGe transistors. The currently available SiGe processes offer
467 130 nm CMOS at a minimum. Transistors faster than 25 GHz have little signal to noise or power
468 improvements to offer when designing readout systems for signals in the 1-2 GHz regime ultra-fast
469 silicon detectors operate in. Moving to faster and smaller SiGe transistors may only introduce
470 unnecessary design challenges such as poor transistor matching, low breakdown voltages, higher
471 Vbe, etc. The current prototype is designed in a 10 GHz process. Significant R&D efforts would be
472 required to determine how much timing resolution, power consumption and dead time performance
473 could be improved by moving to a specific 20-30 GHz process.

474 **3.4 Full digitization chip**

475 University of California Santa Cruz is currently working with Nalu Scientific to design and fabricate
476 a high channel density and scalable radiation-hard waveform digitization ASIC with embedded
477 interface to advanced high-speed sensor arrays such as e.g. AC-LGADs. The chip is being fabricated
478 with TSMC's 65nm technology using design principles consistent with radiation hardening and
479 targets the following features: picosecond-level timing resolution; 10 Gs/s waveform digitization
480 rate to allow pulse shape discrimination; moderate data buffering (256 samples/chnl); autonomous
481 chip triggering, readout control, calibration and storage virtualization; on-chip feature extraction
482 and multi-channel data fusion; reduced cost and increased reliability due to embedded controller
483 (reduction of external logic). Existing readout approaches, such as ALTIROC and the newer
484 TimeSPOT1, promise good-to-excellent timing resolution and channel density, and use a TDC-
485 based measurement for signal arrival times and time-over-threshold (ToT) for an indirect estimate
486 of integrated charge. However, these readout strategies will likely adversely impact the ability to
487 provide sub-pixel spatial resolution and are typically have difficulty compensating for environmental
488 factors such as pile-up, sensor aging, and radiation; timing precision can also be adversely impacted
489 by factors such as timewalk, baseline wander and waveform shape variations. Here, instead, full
490 waveform digitization will be used, which is expected to be more robust against a variety of adverse
491 factors which can affect timing and spatial precision. The initial iteration of the readout chip
492 (v1) was recently (Jan 2022) fabricated for 50 um AC-LGADs. Later versions of the chip will
493 be designed for 20 um pixel arrays and also test the minimum pitch feasible for a single-channel
494 readout using a one-to-one pixel-input channel mapping. The final version of the chip will feature
495 a transimpedance amplifier input stage able to be fine-tuned (or tunable) in order to accommodate
496 high-density sensor arrays using technologies other than AC-LGADs.

497 **3.5 28nm CMOS technology TDC design**

498 CERN's EP RD WP5: CMOS Technologies [48] survey has promoted the selection of 28nm CMOS
499 node as the next step in microelectronics scaling for HEP designs. The choice was based on
500 radiation-hardness studies [49], frequency and cost of MPW runs and strong presence on the market.
501 Furthermore, the 28nm technology is at least twice as fast and allows circuit densities around 4-5
502 times higher than the previously employed 65nm node, making it a good candidate for design of

503 high granularity 4D trackers. One of the critical circuit blocks necessary to enable 4D operation
504 in trackers are low-power and compact Time-to-Digital Converters (TDC) capable of high time-
505 measurement precision. SLAC has stated the design of TDCs in 28nm technology node with target
506 time resolutions of 10-50ps. The plan is to submit the first prototype for fabrication at the end of
507 this year.

508 3.6 Chips comparison

509 Write something about the different approach performances

510 4 Layout

511 A major next step towards 4D tracking at future hadron colliders is the study of how to best
512 combine timing with spatial information. The fine spatial tracking resolution demand towards
513 small pixel with low material budget and low power may make it impractical to instrument finest
514 timing capabilities on all layers. On the other hand, 4D devices with still fine spatial granularity
515 and integrated some coarse timing capabilities can potentially allow a versatile mixture of layers
516 with different balance of spatial and timing resolution to serve an optimal overall 4D tracking for
517 the wide range of applications. The addition of timing information to every pixel hit might not be
518 the approach that leads to the best performance. Alternative approaches such as alternating spatial
519 with timing layers, or 4D with 3D layers could help improve the overall physics performance.

520 Another aspect of detector layout is related to the physics drivers motivating its development.
521 For example, improved and fast charged track reconstruction, heavy flavor (b/c) tagging, and
522 particle-flow reconstruction under very high pileup density will require 4D information in the inner
523 layers, whereas LLP and time-of-flight particle ID capabilities, including the possibility of strange-
524 tagging [50–53], will benefit from 4D information in the outer layers. LLP applications would
525 demand continuous timing coverage and could benefit from modest timing resolution in more layers
526 without stretching timing dynamic range. Future e^+e^- collider vertex detector backgrounds are
527 predominantly back-scattered bremsstrahlung particles from downstream magnets and collimators
528 with \sim ns range delays. 4D tracking devices with fine spatial resolution and modest timing resolution
529 in other layers could significantly enhance the overall performance.

530 Other key considerations are tracking material and pseudorapidity coverage. The additional
531 material required to go from 3D to 4D tracking will have an impact on the track-time association
532 efficiency and mis-association rate. Whereas a lower track-time efficiency will simply reduce the
533 potential gains from timing information, the wrong assignment of times to tracks is particularly
534 problematic as in this case the 4D reconstruction will perform worse than 3D. The impact of
535 showering of particles within the tracking material might be partially mitigated with the use of
536 advanced algorithms based on graph neural networks or other deep learning techniques but this
537 will require a long term study. In the case of future lepton colliders, material in the tracking
538 detector has to be minimized to not degrade p_t and impact parameter resolution, posing additional
539 constrains on the incorporation timing information [?]

540 5 Key areas for future R&D

541 Ariel Schwartzman, Simone Mazza, Su Dong, + additional contributors

542 Valentina: Maybe something of what is written above for ATLAS could go here? Or we can
543 highlight there already that this is a key area for future R&D, making a sort of recommendation

544 to the particle physics community.

545 **6 Summary**

546 Need executive summary 1 page

References

- [1] Technical Design Report: A High-Granularity Timing Detector for the ATLAS Phase-II Upgrade. Technical Report CERN-LHCC-2020-007. ATLAS-TDR-031, CERN, Geneva, Jun 2020.
- [2] Collaboration CMS. A MIP Timing Detector for the CMS Phase-2 Upgrade. Technical Report CERN-LHCC-2019-003. CMS-TDR-020, CERN, Geneva, Mar 2019.
- [3] Hartmut F-W Sadrozinski, Abraham Seiden, and Nicolò Cartiglia. 4D tracking with ultra-fast silicon detectors. *Reports on Progress in Physics*, 81(2):026101, dec 2017.
- [4] Jia Liu, Zhen Liu, and Lian-Tao Wang. Enhancing Long-Lived Particles Searches at the LHC with Precision Timing Information. *Physical Review Letters*, 122(13), Apr 2019.
- [5] Technical Design Report for the ATLAS Inner Tracker Pixel Detector. Technical Report CERN-LHCC-2017-021. ATLAS-TDR-030, CERN, Geneva, Sept 2017.
- [6] Technical Design Report for the ATLAS Inner Tracker Strip Detector. Technical Report CERN-LHCC-2017-005. ATLAS-TDR-025, CERN, Geneva, Apr 2017.
- [7]
- [8] Zbynek Drasal. Status and Challenges of Tracker Design for FCC-hh. *PoS, Vertex 2017:030*. 10 p, 2018.
- [9] Ties Behnke, James E. Brau, Brian Foster, Juan Fuster, Mike Harrison, James McEwan Paterson, Michael Peskin, Marcel Stanitzki, Nicholas Walker, and Hitoshi Yamamoto. The international linear collider technical design report - volume 1: Executive summary, 2013.
- [10] M. Breidenbach, J. E. Brau, P. Burrows, T. Markiewicz, M. Stanitzki, J. Strube, and A. P. White. Updating the sid detector concept, 2021.
- [11] The ILD Collaboration. International large detector: Interim design report, 2020.
- [12] Sukeerthi Dharani. Particle Identification using Time of Flight in the International Large Detector ILD. Bachelorarbeit, Universität Leipzig, 2018. This bachelor thesis has been carried out at DESY and submitted to Universität Leipzig for graduation.; Bachelorarbeit, Universität Leipzig, 2018.
- [13] Lucie Linssen, Akiya Miyamoto, Marcel Stanitzki, and Harry Weerts. Physics and detectors at clic: Clic conceptual design report, 2012.
- [14] Dominik Arominski, Jean-Jacques Blaising, Erica Brondolin, Dominik Dannheim, Konrad Elsener, Frank Gaede, Ignacio García-García, Steven Green, Daniel Hynds, Emilia Leogrande, Lucie Linssen, John Marshall, Nikiforos Nikiforou, Andreas Nürnberg, Estel Perez-Codina, Marko Petrič, Florian Pitters, Aidan Robson, Philipp Roloff, André Sailer, Ulrike Schnoor, Frank Simon, Rosa Simoniello, Simon Spannagel, Rickard Ström, Oleksandr Viazlo, Matthias Weber, and Boruo Xu. A detector for clic: main parameters and performance, 2018.
- [15] Yuri Alexahin et al. The Case for a Muon Collider Higgs Factory. In *Community Summer Study 2013: Snowmass on the Mississippi*, 7 2013.
- [16] K. Long, D. Lucchesi, M. Palmer, N. Pastrone, D. Schulte, and V. Shiltsev. Muon colliders to expand frontiers of particle physics. *Nature Phys.*, 17(3):289, 2021.

- 585 [17] C. Adolphsen et al. European Strategy for Particle Physics – Accelerator R&D Roadmap. 1
586 2022.
- 587 [18] N. V. Mokhov and S. I. Striganov. Detector Background at Muon Colliders. *Phys. Procedia*,
588 37:2015, 2012.
- 589 [19] Armen Tumasyan et al. The Phase-2 Upgrade of the CMS Tracker. 6 2017.
- 590 [20] Muon collider physics and performance working group. To be published in separate White
591 Paper as Muon Collider Detector and Physics Object Reconstruction Performance.
- 592 [21] Nazar Bartosik et al. Detector and Physics Performance at a Muon Collider. *JINST*,
593 15(05):P05001, 2020.
- 594 [22] C. Madrid, R. Heller *et al.* Test Beam Measurements of BNL and HPK AC-LGADs. The 39th
595 RD50 Workshop, 2021.
- 596 [23] M. Tornago, R. Arcidiacono, N. Cartiglia, M. Costa, M. Ferrero, M. Mandurrino, F. Siviero,
597 V. Sola, A. Staiano, A. Apresyan, K. Di Petrillo, R. Heller, S. Los, G. Borghi, M. Boscardin,
598 G.-F. Dalla Betta, F. Ficorella, L. Pancheri, G. Paternoster, H. Sadrozinski, and A. Seiden.
599 Resistive ac-coupled silicon detectors: Principles of operation and first results from a combined
600 analysis of beam test and laser data. *Nucl. Instrum. Methods. Phys. Res. A*, 1003, 2021.
- 601 [24] A. Apresyan, W. Chen, G. D'Amen, K.F. Di Petrillo, G. Giacomini, R. Heller, H. Lee, C.-S.
602 Moon, and A. Tricoli. Measurements of an AC-LGAD strip sensor with a 120 GeV proton
603 beam. *J. Instrum.*, 15(09), 2020.
- 604 [25] S. Mazza. <https://indico.cern.ch/event/1029124/contributions/4410388/>.
- 605 [26] G. Paternoster, G. Borghi, M. Boscardin, N. Cartiglia, M. Ferrero, F. Ficorella, F. Siviero,
606 A. Gola, and P. Bellutti. Trench-isolated low gain avalanche diodes (ti-lgads). *IEEE Electron*
607 *Device Letters*, 41(6):884–887, 2020.
- 608 [27] S. Ayyoub, C. Gee, R. Islam, S. M. Mazza, B. Schumm, A. Seiden, and Y. Zhao. A new
609 approach to achieving high granularity for silicon diode detectors with impact ionization gain.
610 1 2021.
- 611 [28] V. Sola, Silicon Sensors for Extreme Fluences. <https://indico.cern.ch/event/813597/contributions/3727861/>.
- 612 [29] S. Mazza, RD on LGAD Radiation Tolerance: the HL-LHC and Beyond.
613 <https://agenda.hep.wisc.edu/event/1391/session/12/contribution/60>.
- 614 [30] N. Cartiglia, Future silicon trackers: 4D tracking, very high fluences, very small pixels.
615 <https://indico.desy.de/indico/event/24272/session/0/contribution/13/material/slides/0.pdf>.
- 616 [31] S.I. Parker, C.J. Kenney, and J. Segal. 3d — a proposed new architecture for solid-state radia-
617 tion detectors. *Nuclear Instruments and Methods in Physics Research Section A: Accelerators,*
618 *Spectrometers, Detectors and Associated Equipment*, 395(3):328–343, 1997. Proceedings of the
619 Third International Workshop on Semiconductor Pixel Detectors for Particles and X-rays.
- 620 [32] M. M. Obertino. The PPS tracking system: performance in LHC Run2 and prospects for LHC
621 Run3. *JINST*, 15(05):C05049, 2020.

- 622 [33] B. Abbott et al. Production and Integration of the ATLAS Insertable B-Layer. *JINST*,
623 13(05):T05008, 2018.
- 624 [34] J. Lange, G. Giannini, S. Grinstein, M. Manna, G. Pellegrini, D. Quirion, S. Terzo, and
625 D. Vázquez Furelos. Radiation hardness of small-pitch 3d pixel sensors up to a fluence of
626 3×10^{16} neq/cm². *Journal of Instrumentation*, 13(09):P09009–P09009, sep 2018.
- 627 [35] Maria Manna, Chiara Grieco, Sebastian Grinstein, Salvador Hidalgo, Giulio Pellegrini, David
628 Quirion, and Stefano Terzo. First characterisation of 3d pixel detectors irradiated at extreme
629 fluences. *Nuclear Instruments and Methods in Physics Research Section A: Accelerators, Spec-*
630 *trometers, Detectors and Associated Equipment*, 979:164458, 2020.
- 631 [36] L. Anderlini, M. Aresti, A. Bizzeti, M. Boscardin, A. Cardini, G.-F. Dalla Betta, M. Ferrero,
632 G. Forcolin, M. Garau, A. Lai, A. Lampis, A. Loi, C. Lucarelli, R. Mendicino, R. Mulargia,
633 M. Obertino, E. Robutti, S. Ronchin, M. Ruspa, and S. Vecchi. Intrinsic time resolution of 3d-
634 trench silicon pixels for charged particle detection. *Journal of Instrumentation*, 15(09):P09029–
635 P09029, sep 2020.
- 636 [37] Davide Brundu et al. Accurate modelling of 3D-trench silicon sensor with enhanced timing
637 performance and comparison with test beam measurements. *JINST*, 16(09):P09028, 2021.
- 638 [38] J Albert et al. Prototype ATLAS IBL Modules using the FE-I4A Front-End Readout Chip.
639 *JINST*, 7:P11010, 2012.
- 640 [39] Lorenzo Piccolo, Sandro Cadeddu, Luca Frontini, Adriano Lai, Valentino Liberali, Angelo
641 Rivetti, and Alberto Stabile. First Measurements on the Timespot1 ASIC: a Fast-Timing,
642 High-Rate Pixel-Matrix Front-End. 1 2022.
- 643 [40] W. Shockley. Currents to conductors induced by a moving point charge. *J. Appl. Phys.*,
644 9(10):635–636, 1938.
- 645 [41] Simon Ramo. Currents induced by electron motion. *Proc. Ire.*, 27:584–585, 1939.
- 646 [42] Ronald Lipton and Jason Theiman. Fast timing with induced current detectors. *Nucl. Instrum.*
647 *Meth. A*, 945:162423, 2019.
- 648 [43] D. Berry and R. Lipton. Simulation and Measurement of the Shockley–Ramo Current from a
649 Pixelated Silicon Detector. <https://indico.fnal.gov/event/46746/contributions/210260/>, 2019.
- 650 [44] B. Markovic et al. ALTIROC1, a 20 ps time-resolution asic prototype for the atlas high gran-
651 ularity timing detector HGTD. *2018 IEEE Nuclear Science Symposium and Medical Imaging*
652 *Conference Proceedings (NSS/MIC), Sydney, Australia*, page 1–3, Dec 2018.
- 653 [45] F. Cenna, N. Cartiglia, A. Di Francesco, J. Olave, M. Da Rocha Rolo, A. Rivetti, J.C. Silva,
654 R. Silva, and J. Varela. TOFFEE: a full custom amplifier-comparator chip for timing applica-
655 tions with silicon detectors. *Journal of Instrumentation*, 12(03):C03031–C03031, mar 2017.
- 656 [46] E.J. Olave, F. Fausti, N. Cartiglia, R. Arcidiacono, H.F.-W. Sadrozinski, and A. Seiden. Design
657 and characterization of the fast chip: a front-end for 4d tracking systems based on ultra-
658 fast silicon detectors aiming at 30 ps time resolution. *Nuclear Instruments and Methods in*
659 *Physics Research Section A: Accelerators, Spectrometers, Detectors and Associated Equipment*,
660 985:164615, 2021.

- 661 [47] A. Rojas, FAST2: a new family of front-end ASICs to read out
662 thin Ultra-Fast Silicon detectors achieving picosecond time resolution.
663 <https://indico.cern.ch/event/1019078/contributions/4443951/>.
- 664 [48] Strategic RD Programme on Technologies for Future Experiments - Annual Report 2020.
665 Technical Report CERN-EP-RDET-2021-001, CERN, Geneva, Apr 2021.
- 666 [49] Giulio Borghello, “Ionizing Radiation Effects On 28 nm CMOS Technology”. Technical report,
667 CERN, Geneva, May 2020.
- 668 [50] SLD Collaboration: Abe, Koya et al. First direct measurement of the parity-violating coupling
669 of the z^0 to the s -quark. *Physical Review Letters*, 85(24):5059–5063, Dec 2000.
- 670 [51] Yuichiro Nakai, David Shih, and Scott Thomas. Strange jet tagging, 2020.
- 671 [52] J. Erdmann. A tagger for strange jets based on tracking information using long short-term
672 memory. *Journal of Instrumentation*, 15(01):P01021–P01021, Jan 2020.
- 673 [53] M.J. Basso, V.M.M. Cairo, U. Heintz, J. Luo, M. Narain, R. S. Orr, A. Schwartzman, D. Su,
674 E. Usai, C. Vernieri, and C. Young. Strange Quark as a probe for new physics in the Higgs
675 Sector. *LoI for Snowmass2021*, 2020.